International Communications in Heat and Mass Transfer 55 (2014) 113–120

Contents lists available at ScienceDirect

International Communications in Heat and Mass Transfer

journal homepage: www.elsevier.com/locate/ichmt

A lattice Boltzmann simulation of enhanced heat transfer of nanofluids ☆

W.N. Zhou [a], Y.Y. Yan [a,*], J.L. Xu [b]

[a] Energy & Sustainability Research Division, Faculty of Engineering, University of Nottingham, University Park, Nottingham NG7 2RD, UK
[b] School of Energy, Power and Mechanical Engineering, North China Electric Power University, Beijing 102206, China

ARTICLE INFO

Available online 2 May 2014

Keywords:
Nanofluids
Heat transfer enhancement
Numerical modelling
Lattice Boltzmann method

ABSTRACT

Due to its distinctive characteristics nanofluid has drawn much attention from academic communities since the last decade. Compared with conventional fluids, nanofluid has higher thermal conductivity and surface to volume ratio, which enables it to be an effective working fluid in terms of heat transfer enhancement. Recent experimental works have shown that with low nanoparticle concentrations (1–5 vol.%), the effective thermal conductivity of the suspensions can increase by more than 20% for various mixtures. Although many outstanding experimental works have been carried out, the fundamental understanding of nanofluid characteristics and performance is still not sufficient. Much more theoretical and numerical studies are required. Over the past two decades, the lattice Boltzmann method (LBM) has experienced a rapid development and well accepted as a useful method to simulate various fluid behaviours. In the present study, the LBM is employed to investigate the characteristics of nanofluid flow and heat transfer. By coupling the density and temperature distribution functions, the hydrodynamics and thermal features of nanofluids are properly simulated. The effects of the parameters including Rayleigh number and volume fraction of nanoparticles on hydrodynamic and thermal performances are investigated. The results show that both Rayleigh number and solid volume fraction of nanoparticles have influences on heat transfer enhancement of nanofluids; and there is a critical value of Rayleigh number on the performance of heat transfer enhancement.

1. Introduction

The commonly used fluids in engineering, such as water and oil, have a primary limitation in enhancing the performance of heat transfer due to their low thermal conductivities. Nanofluids, using nanoparticles dispersed in a base fluid, have been proposed recently to overcome this drawback. Nanofluids have distinguished thermal features such as high surface to volume ratio, resulting in their perfect thermal performance. Thus, nanofluids are considered as an effective approach to meet some challenges associated with the conventional microfluids.

Many researchers have experimentally studied flow and thermal characteristics of nanofluids in recent years. Teng *et al.* [1] examined the influence of weigh fraction, temperature, and particle size on the thermal conductivity of Al_2O_3/water nanofluids. Experimental works [2] reported that with low nanoparticle concentration (1–5 vol.%), the effective thermal conductivity of the suspensions can increase by more than 20% for various mixtures. Oztop *et al.* [3] studied the effect of the position and the aspect ratio of a thin heated plate on free convection in a cavity to find that Nu increases with Ra and concluded that the enhancement is more pronounced for the vertical plate. Nguyen *et al.* [4] studied the viscosity of Al_2O_3/water nanofluid and found that for higher particle fractions, viscosities of 47 nm particle-size are clearly higher than those of 36 nm. Much more specific works on nanofluids can be seen in the recent review papers [5,6].

Meanwhile, nanofluids are also theoretically and numerically investigated by many researchers. Khanafer *et al.* [7] numerically investigated buoyancy-driven heat transfer enhancement in a 2D enclosure utilizing nanofluids by using finite-volume approach. Their results showed that the heat transfer rate of the nanofluid increases with the volume fraction of the nanoparticle. Raisi *et al.* [8] numerically studied the thermal performance of a micro-channel cooled by Cu/water nanofluids and it was indicated that the heat transfer rate is significantly affected by the solid volume fraction and slip velocity coefficient at high Reynolds numbers. Heris *et al.* [9] used a dispersion model to investigate laminar flow convective heat transfer of nanofluid in a circular tube. Their results clearly showed that the addition of nanoparticles to the base liquid produces considerable enhancement of heat transfer. The lattice Boltzmann method (LBM), which is obtaining more attention and popularity [10–12], is applied in many areas of computational fluid dynamics, including multiphase flows [13,14], electro-osmotic flows [15,16], and heat transfer characteristics [17–19]. Based on a meso-scope model, LBM has many advantages over conventional CFD approaches [20–22]. Generally speaking, LBM is much easier to implement, more

☆ Communicated by W.J. Minkowycz.
* Corresponding author.
E-mail address: yuying.yan@nottingham.ac.uk (Y.Y. Yan).

http://dx.doi.org/10.1016/j.icheatmasstransfer.2014.04.010
0735-1933/

Nomenclature

c	lattice speed
c_i	discrete particle speeds
c_s	speed of sound
c_p	specific heat capacity
f_i	density distribution function
f^{eq}	equilibrium distribution function of f_i
F_i	forcing term
g	gravitational acceleration
g_i	energy distribution function
k	effective thermal conductivity
L	enclosure length
Ma	Mach number
Nu	Nusselt number
Pr	Prandtl number
Ra	Rayleigh number
T	temperature
w_i	weighting factor

Greek symbols

τ	relaxation time
ρ	density
φ	nanoparticle volume fraction, dimensionless
μ	dynamic viscosity
ν	kinetic viscosity
α	thermal diffusivity

computationally efficient and more capable to deal with complex boundary conditions and interactions between different phases. LBM has been widely chosen to simulate phenomena of nanofluid heat transfer. Xuan and Yao [19] proposed a lattice Boltzmann model to simulate flow and energy transport processes inside the nanofluids by accounting for the external and internal forces. Yang and Lai [23] studied forced convection Al_2O_3/water flow in a microchannel using the lattice Boltzmann method. Their results indicated that the average Nusselt number increases with Reynolds number and particle volume concentration. He *et al.* [18] developed a lattice Boltzmann model to simulate the convection heat transfer utilizing Al_2O_3/water nanofluids in a square cavity. Their work indicated that the flow and heat transfer characteristics of Al_2O_3/water nanofluid in the square cavity are more sensitive to viscosity than to thermal conductivity. Other numerical schemes were also employed to investigate nanofluids. Finite volume method was adopted by Abu-Nada *et al.* [24] to study the nanoparticle influences on heat transfer enhancement in horizontal annuli. A finite difference approach was applied by Jou and Tzeng [25] to simulate natural convection in a rectangular cavity with different aspect ratios. Though some numerical studies have been done over the past few years, there is still a lack of fundamental understanding of the effect of thermo-physical parameters on the heat transfer performance. In the present study, a lattice Boltzmann model coupling the density and the temperature distribution functions is proposed to simulate heat transfer utilizing nanofluids in a square cavity. The effects of several thermo-physical parameters including Rayleigh number and nanoparticle volume fraction on heat transfer performance are investigated.

2. Mathematical formulation

2.1. Lattice Boltzmann method

The lattice Boltzmann method is employed in this work along with the application of the standard D2Q9 for both velocity and temperature field. The details about the lattice Boltzmann method have already been given in many references [12,26,27] only a brief induction will be given in the present paper. The lattice Boltzmann method is carried out through two basic steps including the collision step and the streaming step, which can be written by the following form:

$$f_i(x + c_i\Delta t, t + \Delta t) = f_i(x,t) - \frac{1}{\tau}\left(f_i(x,t) - f_i^{eq}(x,t)\right) + \Delta t F_i \tag{1}$$

where τ is the dimensional relaxation time, $f_i(x, t)$ is the density distribution function for the particle moving with velocity c_i at position x and time t, and $f_i^{eq}(x, t)$ is the local equilibrium distribution function. F_i is the external force term in the direction of lattice velocity. For the typical two-dimensional nine-speed (D2Q9) lattice scheme considered in the present work, the local equilibrium distribution function is defined as:

$$f_i^{(eq)} = \rho w_i\left[1 + \frac{c_i \cdot u}{c_s^2} + \frac{(c_i \cdot u)^2}{2c_s^4} - \frac{u \cdot u}{2c_s^2}\right] \tag{2}$$

where w_i is the weighting factor, given as 4/9 for $i = 0$, 1/9 for $i = 1, 2, 3$, 4, and 1/36 for $i = 5, 6, 7, 8$. c_s is the sound speed. c_i is the discrete velocities, and defined as:

$$c_i = \begin{cases} (0,0), i = 0 \\ c(\cos\theta_i, \sin\theta_i), (\theta_i = (i-1)\pi/2, i = 1,2,3,4) \\ \sqrt{2}c(\cos\theta_i, \sin\theta_i), (\theta_i = (i-5)\pi/2 + \pi/4, i = 5,6,7,8) \end{cases} \tag{3}$$

where $c = \Delta x/\Delta t$ is the particle streaming speed. Δx and Δt are the lattice spacing and time step. The relation between c_s and c can be expressed as $c_s = c/\sqrt{3}$. The macroscopic variables such as the mass density, the momentum density and the pressure are defined by sums over the distribution functions:

$$\rho = \sum_i f_i, \rho u = \sum_i f_i c_i, p = \frac{c^2}{3}\rho \tag{4}$$

The kinematic viscosity is determined by:

$$\nu = (\tau - 1/2)c_s^2\Delta t \tag{5}$$

For the scalar function (temperature in this study), another distribution is defined as:

$$g_i(x + c_i\Delta t, t + \Delta t) = g_i(x,t) - \frac{1}{\tau}\left(g_i(x,t) - g_i^{eq}(x,t)\right) \tag{6}$$

The equilibrium distribution function can be written as:

$$g_i^{(eq)} = w_i T\left[1 + \frac{c_i \cdot u}{c_s^2}\right] \tag{7}$$

The macroscopic temperature is calculated as follow:

$$T = \sum_i g_i \tag{8}$$

The thermal diffusivity is related to the relaxation time by:

$$\alpha = (\tau_c - 1/2)c_s^2\Delta t \tag{9}$$

For natural convection, the important dimensionless parameters Prandtl number Pr and Rayleigh number Ra are defined as:

$$\mathrm{Pr} = \nu/\chi \tag{10}$$

$$Ra = g\beta\Delta T L^3\,\mathrm{Pr}/\nu^2 \tag{11}$$

Table 1
Thermo-physical properties of different phases of Al_2O_3/water nanofluids.

Properties	Base fluid (water)	Nanoparticles (Al_2O_3)
ρ (kg/m3)	997.1	3970
c_p (J/kg K)	4179	765
μ (kg/m s)	0.001004	/
$\beta \times 10^5$ (1/K)	21	0.85
k(W/m K)	0.613	25

where ΔT is the temperature difference between the high temperature wall and low temperature wall. L is the characteristic length of the square cavity.

Another dimensionless parameter Mach number Ma is defined as:

$$Ma = u_c/c_s \tag{12}$$

where $u_c = \sqrt{g\beta\Delta TL}$ is the characteristic velocity of natural convection. Considering that LBE applies in incompressible limit, Mach number should be less than 0.3. In the present study, Mach number was fixed at $Ma = 0.1$.

In the simulation the Boussinessq approximation is applied to the buoyancy force term. In that case, the buoyancy force term is added as an extra source term to Eq. (1) by:

$$F_i = 3w_i g\beta\Delta T \tag{13}$$

In the lattice Boltzmann model, real quantities such as space and time need to be converted to lattice units prior to simulation. By introducing characteristic scales, the dimensionless process can be accomplished. To make sure that the simulation case represents the relevant practical phenomenon, non-dimensional quantities such as Reynolds number remain the same in the dimensionless process.

2.2. Lattice Boltzmann model for nanofluid

In this paper, the nanofluid is assumed similar to a single phase fluid. Hence, the equations of physical parameters of the nanofluid are as follows:

Density equation:

$$\rho_{nf} = (1-\phi)\rho_f + \phi\rho_p \tag{14}$$

where ρ_{nf} is the density of nanofluid, ρ_f is the density of base fluid and ρ_p is the density of nanoparticle. ϕ is the volume fraction of nanoparticles.

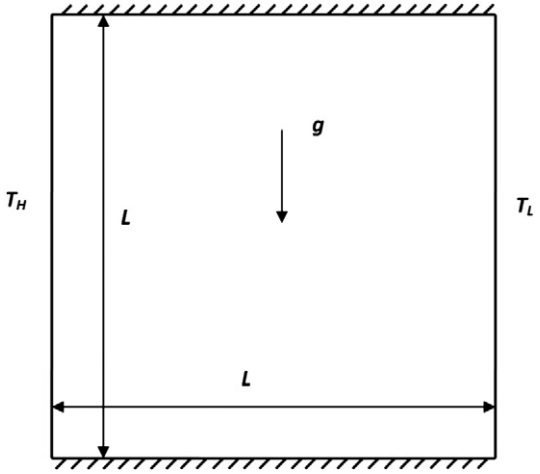

Fig. 1. Schematic domain of the physical model.

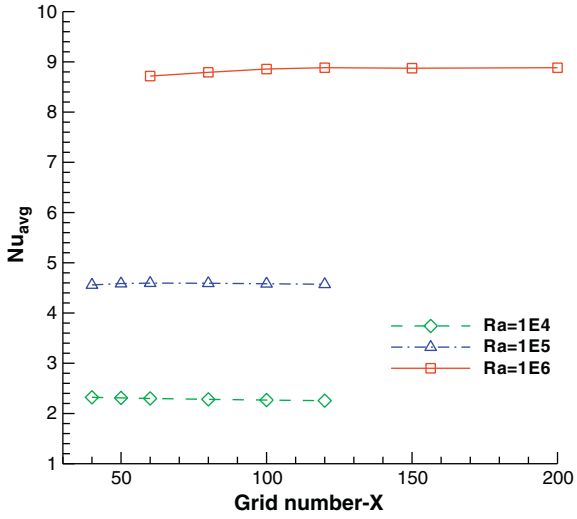

Fig. 2. Grid independent test: Nu_{avg} versus grid number (4% Al_2O_3/water nanofluid).

Heat capacity equation is expressed by:

$$\left(\rho c_p\right)_{nf} = (1-\phi)\left(\rho c_p\right)_f + \phi\left(\rho c_p\right)_p; \tag{15}$$

and the dynamic viscosity equation is given by:

$$\mu_{nf} = \mu_f/(1-\phi)^{2.5}. \tag{16}$$

The thermal expansion coefficient of the nanofluid can be calculated by:

$$(\rho\beta)_{nf} = (1-\phi)(\rho\beta)_f + \phi(\rho\beta)_p \tag{17}$$

The effective thermal conductivity of the nanofluid can be determined by the Maxwell–Garnetts (MG) model by:

$$\frac{k_{nf}}{k_f} = \frac{k_p + 2k_f - 2\phi\left(k_f - k_p\right)}{k_p + 2k_f + \phi\left(k_f - k_p\right)} \tag{18}$$

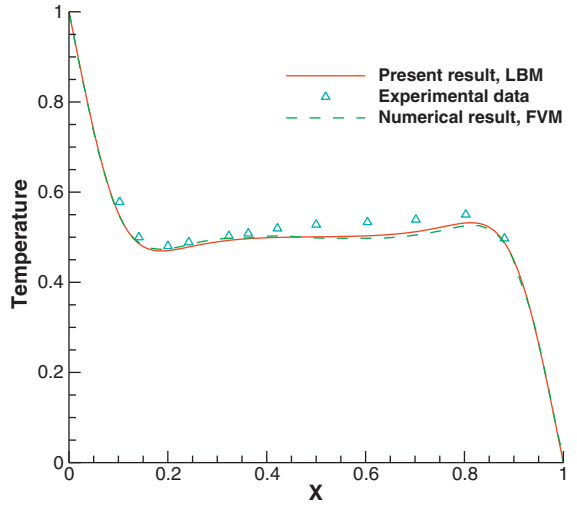

Fig. 3. Comparison with other simulation and experimental results ($Ra = 1.89 \times 10^5$, $Pr = 0.71$).

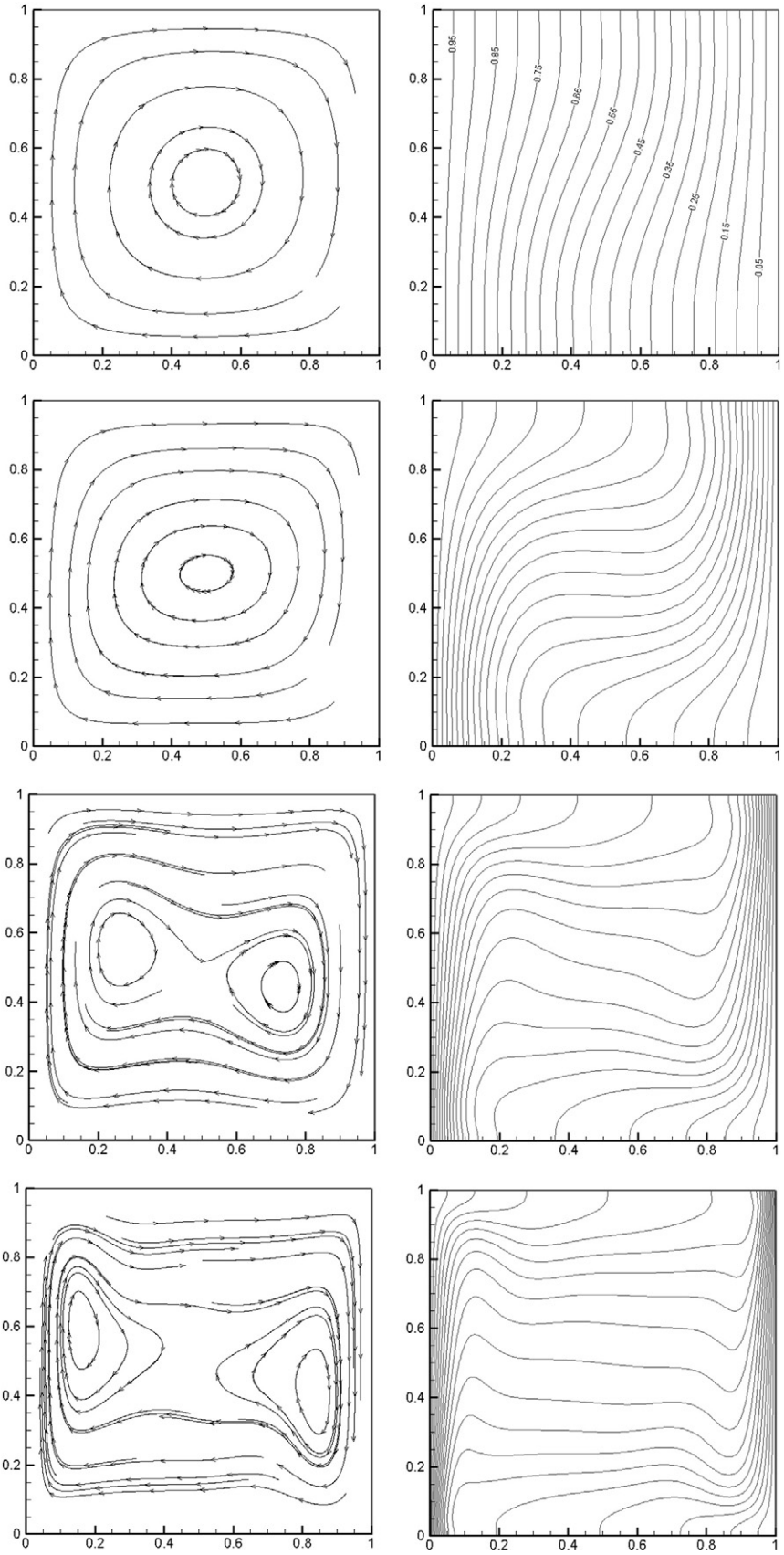

Fig. 4. Comparisons of isotherms and streamlines for 4% Al_2O_3/water nanofluid of $Ra = 1 \times 10^3$–10^6 (top to bottom).

The local Nusselt number and the average value at the hot and cold walls are calculated as:

$$Nu_y = -\frac{H}{\Delta T}\frac{\partial T}{\partial x} \tag{19}$$

$$Nu_{avg} = \frac{1}{H}\int_0^H Nu_y dy \tag{20}$$

where H is the height of the square, ΔT is the temperature difference between the hot and cold walls. For convenience, a normalized average Nusselt number is defined as the ratio of Nusselt number at any volume fractions of nanoparticles to that of pure water, which is as follows:

$$Nu^*_{avg}(\varphi) = Nu_{avg}(\varphi)/Nu_{avg}(\varphi = 0) \tag{21}$$

2.3. Boundary treatments

The implementation of boundary conditions is very important for LBM simulations. The unknown distribution functions pointing to the fluid zone at the boundary nodes must be specified after every iteration step. Concerning the no-slip boundary condition, the bounce back boundary condition is employed on the solid boundaries.

The top and bottom of the boundaries are adiabatic so the bounce back boundary condition is employed. Temperatures at the left and right walls are known. Since we are using D2Q9, for the left wall, the unknown distribution functions are evaluated as:

$$g_1 = T_H(w(1) + w(3)) - g_3$$
$$g_5 = T_H(w(5) + w(7)) - g_7$$
$$g_8 = T_H(w(8) + w(6)) - g_6$$

The unknown distribution functions can be obtained in the similar way at the right wall.

3. Results and discussion

The problem considered in this study is a natural convection in a two dimensional square cavity with sidewalls maintained at different temperatures and driven by the buoyancy force. The thermo-physical properties of water and Al_2O_3 nanoparticle are given in Table 1. The properties of Al_2O_3/water nanofluids are obtained by the equations given in the previous section. The square cavity used in this study is shown in Fig. 1. The height and the width of the enclosure are given by L. The temperatures of the two sidewalls of the cavity are maintained

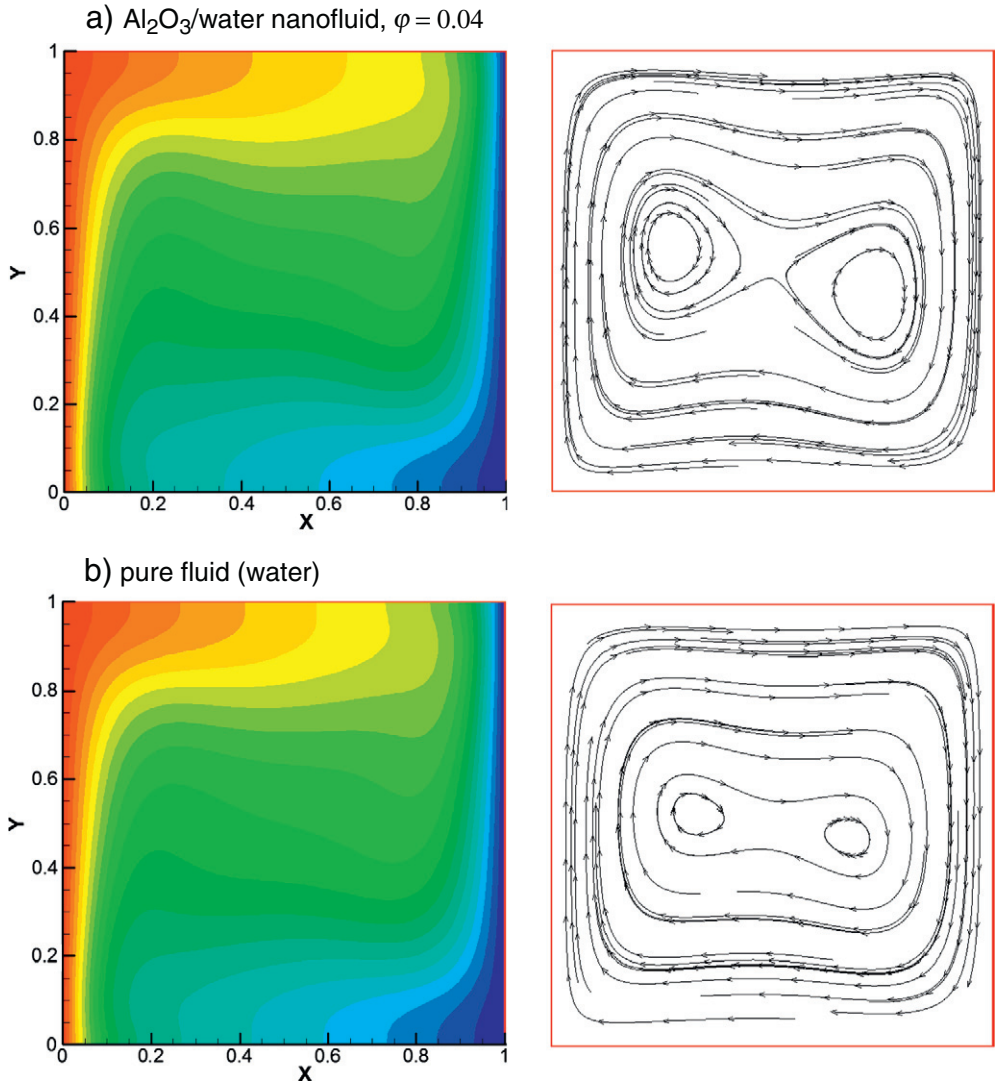

Fig. 5. Comparisons of isotherms and streamlines for 4% Al_2O_3/water nanofluid and pure fluid, $Ra = 1 \times 10^5$.

at T_H and T_L, where $T_H > T_L$. The boundary conditions of the top and bottom walls are adiabatic. The boundary conditions of the four walls are given as:

$$u = v = 0, T = T_H \ for \ x = 0;$$
$$u = v = 0, T = T_L \ for \ x = L;$$
$$u = v = 0, \partial T/\partial y = 0 \ for \ y = 0;$$
$$u = v = 0, \partial T/\partial y = 0 \ for \ y = L.$$

To ensure that the solution is grid independent, an extensive mesh testing procedure was conducted. Calculations of different mesh cases were carried out for 4% Al_2O_3/water nanofluid of $Ra = 1 \times 10^4$, 1×10^5 and 1×10^6, respectively. The average Nusselt numbers were calculated and the grid independence is ensured; see Fig. 2. It should be noted that the viscosity can be obtained by Eqs. (11) and (12) by fixing Rayleigh number, Prandtl number and Mach number. It can be seen that the lattice number has a positive impact to the viscosity in the lattice Boltzmann model. To keep the relaxation times in a suitable range for both flow dynamics and thermal evolution in the lattice Boltzmann model, the lattice number is particularly considered and different meshes for different cases are also considered. In the present study, 100×100 lattices are chosen for Rayleigh number less than 1×10^5 and 150×150 lattices for the other cases.

To further validate the proposed lattice Boltzmann model for incompressible fluid, the simulation results were compared not only with the experimental results of Krane and Jessee [28] but also with the numerical work by Khalil Khanafer *et al.* [29] for natural convection in an enclosure filled with air. Fig. 3 shows that the comparisons are in excellent agreement.

After validating the code, the effect of nanoparticles suspended in water is studied. The square enclosure is filled with Al_2O_3/water nanofluid. The geometric dimension of the enclosure in this study is 10 mm × 10 mm. The volume fraction of 47 nm Al_2O_3 nanoparticles is 0 to 5%. The hot wall temperature has been considered as 303 K while the cold wall is 293 K. It should be mentioned that in the lattice Boltzmann model all physical quantities have been dimensionless and rescaled. As long as the characteristic dimensionless numbers are kept constant in the dimensionless conversion, the physical phenomena can be represented by the simulation results.

To investigate the effect of nanoparticle on heat transfer enhancement, a series of simulation cases were carried out with Rayleigh number ranging from 1×10^3 to 10^6 and solid volume fraction 0 to 5%. The streamlines and isotherms of 4% Al_2O_3/water nanofluid with Rayleigh ranging from 1×10^3 to 10^6 have been presented in Fig. 4. The figures show that at low Rayleigh number 1×10^3, the central vortex appears as a dominant characteristic of the fluid flow. With the increase of Rayleigh number, the central vortex tends to become elliptic and eventually breaks up into two vortices at $Ra = 1 \times 10^5$. The thickness of the thermal boundary layer near the wall also decreases with the increase of Rayleigh number. This is due to the increase in buoyancy as the viscosity and density remain the same for a particular volume fraction. The effect of nanoparticle on streamlines and isotherms is also investigated by fixing the Rayleigh number.

Fig. 5 shows the comparisons of isotherms and streamlines for 4% Al_2O_3/water nanofluid and pure water at $Ra = 1 \times 10^5$. In the presence of nanoparticles, the central vortices occupy a larger zone compared with the pure fluid due to the increase of energy transport through the fluid associated with the irregular motion of nanoparticles.

The impact of solid volume fraction on isotherms is shown in Fig. 6. It can be seen from the figure that with the increase in volume fraction, the isotherms become closer to the vertical wall. The thermal layer becomes thinner compared with the pure fluid. It is observed that the increase of solid concentration leads to the enhancement of heat transfer, and such enhancement is due to the increase of the effective thermal conductivity with the increase of solid volume fractions of nanoparticles. However, the effect of heat transfer enhancement decreases with the increase in Rayleigh number, and therefore the solid concentration has a little effect on the thermal distribution. This will be shown in the following discussion.

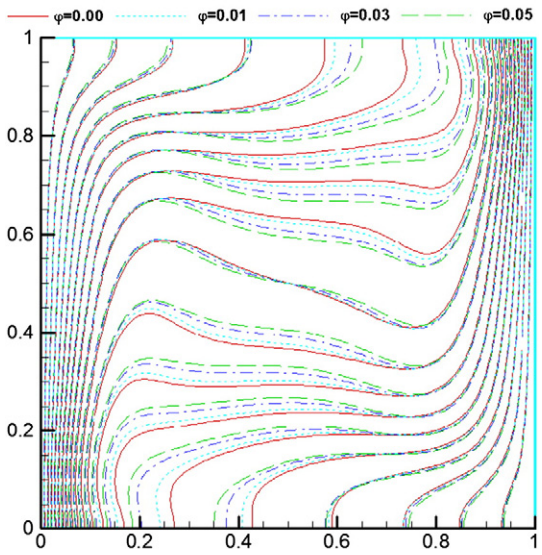

Fig. 6. Comparison of isotherms between base fluid and Al_2O_3/water nanofluid at $Ra = 1 \times 10^5$.

Fig. 7 displays the effect of solid volume fraction on the temperature and vertical component of velocity distribution along the horizontal

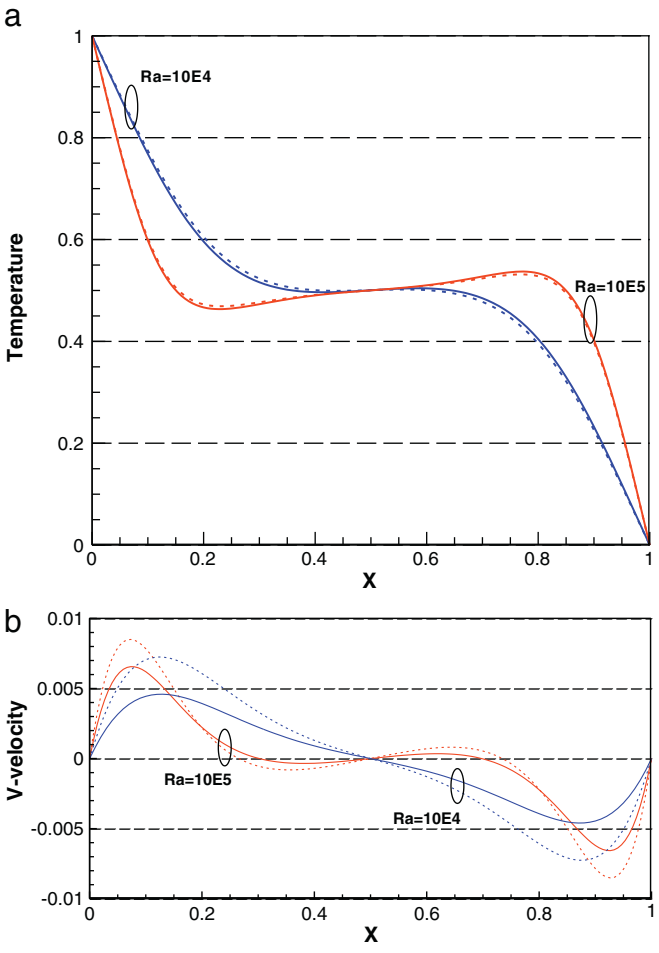

Fig. 7. Comparison of the temperature (a) and velocity profiles (b) between 4% Al_2O_3/water nanofluid (—) and pure fluid (---) at the mid plane.

axis. An increase of temperature gradient in nanofluid is observed compared with pure water for $Ra = 1 \times 10^4$ and 10^5. This leads to a larger local Nusselt number and therefore enhances the heat transfer performance. In addition, the velocity of nanofluid is found larger than that of pure water for the chosen Rayleigh numbers which may cause a stronger convection and consequently result in a larger Nusselt number.

The effect of solid volume fractions on average Nusselt number along the heated wall at various Rayleigh numbers is illustrated in Fig. 8(a). It is found that the average Nusselt numbers increase with solid volume fractions. This is because the added nanoparticles augment the effective thermal conductivity and hence heat transfer. Fig. 8(b) shows the effect of volume fractions on the normalized average Nusselt number. It can be seen that for a fixed Rayleigh number, solid volume fractions can affect the enhancement of heat transfer. However the effect decreases with the increase of Rayleigh number. By adding 5% Al_2O_3 nanoparticles by volume, the normalized Nusselt number increases about 3.8% at $Ra = 1 \times 10^4$, a slight decline to 3.5% at $Ra = 1 \times 10^5$, but decreases significantly to 1.6% when Rayleigh number increases to 1×10^6. This means that there is a critical value of Rayleigh number of Al_2O_3/water nanofluid for the performance of heat transfer enhancement in terms of the normalized average Nusselt number. Similar conclusion was obtained in [30]. Fig. 9 shows comparisons between the pure fluid and nanofluid of the local Nusselt number distribution along the heated wall. It can be seen that the increase of volume fractions increases the local Nusselt number along the heated wall. The influence is more evident at the bottom of the hot wall.

4. Conclusions

In the present study, a lattice Boltzmann model coupling the density and temperature distribution functions is employed to investigate the flow and heat transfer characteristics of Al_2O_3/water nanofluids. The effects of different Rayleigh numbers (1×10^3–10^6) and solid volume fractions (0–5%) on the heat transfer performance of nanofluid are examined and discussed. The conclusions can be summarized as follows:

(1) The addition of nanoparticles into pure water has effects on both hydrodynamic and thermal performances compared with pure water.
(2) At a fixed Rayleigh number, the velocity of nanofluid in the enclosure is larger than that of pure water which causes a stronger convection and hence heat transfer enhancement.

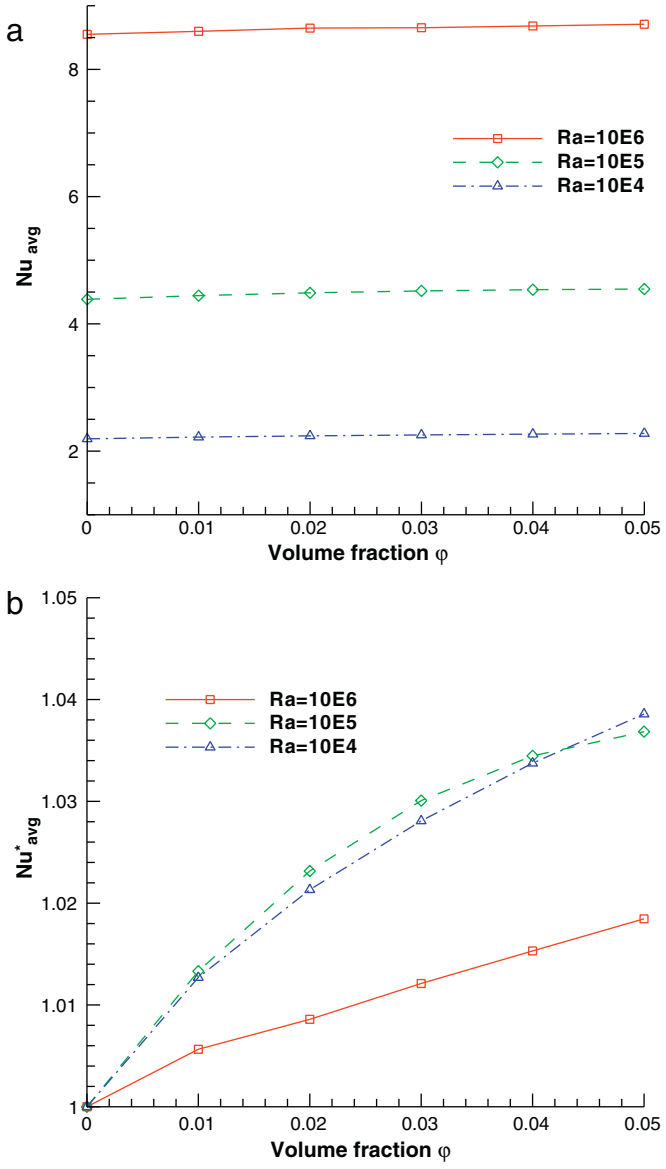

Fig. 8. Average Nusselt numbers (a) and normalized Nusselt numbers (b) with different Rayleigh numbers.

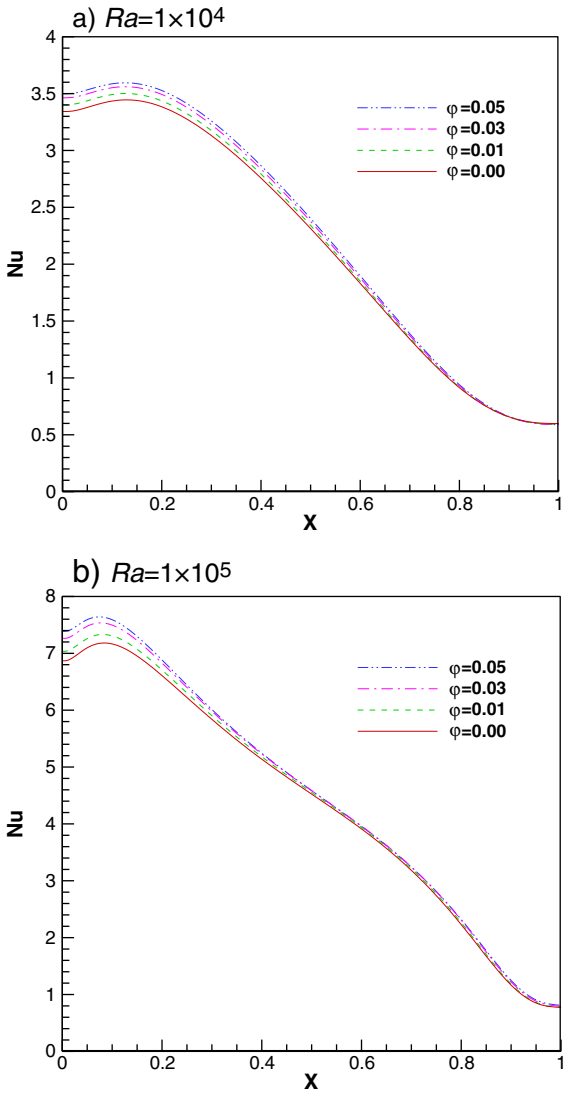

Fig. 9. Nusselt number distributions on the hot wall at different volume fractions and Rayleigh numbers.

(3) The average Nusselt number and normalized average Nusselt number increase with the solid volume fractions because the added nanoparticles augment the effective thermal conductivity and hence heat transfer.
(4) There is a critical Rayleigh number for the performance of heat transfer enhancement of applying nanofluids; beyond the critical value, the enhancement effect will become smaller.

Acknowledgements

The work presented in this article is supported by the scholarship joint sponsored by the University of Nottingham, UK, Faculty of Engineering scholarship (2010–13) and the Chinese Scholarship Council (CSC) scholarship for PhD (2010–13), and also by the Royal Society-NSFC joint project under IE110858 (2012–2014).

References

[1] T.P. Teng, Y.H. Hung, T.C. Teng, H.E. Mo, H.G. Hsu, The effect of alumina/water nanofluid particle size on thermal conductivity, Appl. Therm. Eng. 30 (14–15) (2010) 2213–2218.
[2] M.S. Liu, M. Ching-Cheng Lin, I. Huang, Enhancement of thermal conductivity with carbon nanotube for nanofluids, Int. Commun. Heat Mass 32 (9) (2005) 1202–1210.
[3] H. Oztop, I. Dagtekin, A. Bahloul, Comparison of position of a heated thin plate located in a cavity for natural convection, Int. Commun. Heat Mass 31 (1) (2004) 121–132.
[4] C.T. Nguyen, G. Roy, C. Gauthier, N. Galanis, Heat transfer enhancement using Al_2O_3–water nanofluid for an electronic liquid cooling system, Appl. Therm. Eng. 27 (8) (2007) 1501–1506.
[5] L. Godson, B. Raja, D. Mohan Lal, S. Wongwises, Enhancement of heat transfer using nanofluids—an overview, Renew. Sust. Energ. Rev. 14 (2) (2010) 629–641.
[6] X.Q. Wang, A.S. Mujumdar, Heat transfer characteristics of nanofluids: a review, Int. J. Therm. Sci. 46 (1) (2007) 1–19.
[7] G. Hazi, A. Markus, On the bubble departure diameter and release frequency based on numerical simulation results, Int. J. Heat Mass Transfer 52 (5–6) (2009) 1472–1480.
[8] A. Raisi, B. Ghasemi, S. Aminossadati, A numerical study on the forced convection of laminar nanofluid in a microchannel with both slip and no-slip conditions, Numer. Heat Transf. Part A Appl. 59 (2) (2011) 114–129.
[9] S.Z. Heris, M.N. Esfahany, G. Etemad, Numerical investigation of nanofluid laminar convective heat transfer through a circular tube, Numer. Heat Transf. Part A Appl. 52 (11) (2007) 1043–1058.
[10] Y.Y. Yan, Y.Q. Zu, B. Dong, LBM, a useful tool for mesoscale modelling of single-phase and multiphase flow, Appl. Therm. Eng. 31 (5) (2011) 649–655.
[11] J. Zhang, Lattice Boltzmann method for microfluidics: models and applications, Microfluid. Nanofluid. (2010) 1–28.
[12] S. Chen, G.D. Doolen, Lattice Boltzmann method for fluid flows, Annu. Rev. Fluid Mech. 30 (1998) 329–364.
[13] Y. Zu, Y. Yan, J. Li, Z. Han, Wetting behaviours of a single droplet on biomimetic micro structured surfaces, J. Bionic Eng. 7 (2) (2010) 191–198.
[14] Y.Y. Yan, Y.Q. Zu, A lattice Boltzmann method for incompressible two-phase flows on partial wetting surface with large density ratio, J. Comput. Phys. 227 (1) (2007) 763–775.
[15] Y.Y. Yan, Y.Q. Zu, L. Ren, J.Q. Li, Numerical modelling of electroosmotically driven flow within the micro thin liquid layer near an earthworm surface—a biomimetic approach. Proceedings of the Institution of Mechanical Engineers, Part C, J. Mech. Eng. Sci. 221 (10) (2007) 1201–1210.
[16] B. Li, W.N. Zhou, Y.Y. Yan, C. Tian, Evaluation of electro-osmotic pumping effect on microporous media flow, Appl. Therm. Eng. 60 (1–2) (2013) 449–455.
[17] G.R. Kefayati, S.F. Hosseinizadeh, M. Gorji, H. Sajjadi, Lattice Boltzmann simulation of natural convection in tall enclosures using water/SiO_2 nanofluid, Int. Commun. Heat Mass 38 (6) (2011) 798–805.
[18] Y. He, C. Qi, Y. Hu, B. Qin, F. Li, Y. Ding, Lattice Boltzmann simulation of alumina–water nanofluid in a square cavity, Nanoscale Res. Lett. 6 (1) (2011) 184.
[19] Y.M. Xuan, Z.P. Yao, Lattice Boltzmann model for nanofluids, Heat Mass Transf. 41 (3) (2005) 199–205.
[20] J. Yeomans, Mesoscale simulations: lattice Boltzmann and particle algorithms, Physica A Stat. Theor. Phys. 369 (1) (2006) 159–184.
[21] C.K. Aidun, J.R. Clausen, Lattice-Boltzmann method for complex flows, Annu. Rev. Fluid Mech. 42 (2010) 439–472.
[22] R. Begum, M.A. Basit, Lattice Boltzmann method and its applications to fluid flow problems, Eur. J. Sci. Res. 22 (2) (2008) 216–231.
[23] Y.T. Yang, F.H. Lai, Numerical investigation of cooling performance with the use of Al_2O_3/water nanofluids in a radial flow system, Int. J. Therm. Sci. 50 (2011) 61–72.
[24] E. Abu-Nada, Z. Masoud, A. Hijazi, Natural convection heat transfer enhancement in horizontal concentric annuli using nanofluids, Int. Commun. Heat Mass 35 (5) (2008) 657–665.
[25] R.-Y. Jou, S.-C. Tzeng, Numerical research of nature convective heat transfer enhancement filled with nanofluids in rectangular enclosures, Int. Commun. Heat Mass 33 (6) (2006) 727–736.
[26] X. He, L.S. Luo, Theory of the lattice Boltzmann method: from the Boltzmann equation to the lattice Boltzmann equation, Phys. Rev. E. 56 (6) (1997) 6811–6817.
[27] Y. Qian, D. d'Humieres, P. Lallemand, Lattice BGK models for Navier–Stokes equation, EPL (Europhys. Lett.) 17 (1992) 479.
[28] R. Krane, J. Jessee, Some detailed field measurements for a natural convection flow in a vertical square enclosure, Proc. 1st ASME-JSME Thermal Engineering Joint Conf, 1983, pp. 323–329.
[29] K. Khanafer, K. Vafai, M. Lightstone, Buoyancy-driven heat transfer enhancement in a two-dimensional enclosure utilizing nanofluids, Int. J. Heat Mass Transfer 46 (19) (2003) 3639–3653.
[30] P.J. Dellar, Lattice kinetic schemes for magnetohydrodynamics, J. Comput. Phys. 179 (1) (2002) 95–126.